Journal of Geophysical Research [Atmospheres]

Supporting Information for

Iodine speciation in aerosol

Juan Carlos Gómez Martín[1]*, Alfonso Saiz-Lopez[2], Carlos A. Cuevas[2], Alex R. Baker[3], Rafael fernández[4]

[1] Instituto de Astrofísica de Andalucía, CSIC, 18008, Granada, Spain

[2] Department of Atmospheric Chemistry and Climate, Institute of Physical Chemistry Rocasolano, CSIC, Serrano 119, 28006 Madrid, Spain

[3] Centre for Ocean and Atmospheric Science, School of Environmental Sciences, University of East Anglia, Norwich, UK

[4] Institute for Interdisciplinary Science, National Research Council (ICB-CONICET), FCEN-UNCuyo, Mendoza, 5501, Argentina

*Correspondence to: Juan Carlos Gómez Martín (jcgomez@iaa.es)

Contents of this file

Additional Supporting Information (Files uploaded separately)

Table S1. List of cruises reporting iodine distribution in aerosol size fractions or aerosol iodine speciation (Gomez Martin-t01.docx).
Table S2. Campaigns in coastal and island stations reporting iodine distribution in aerosol size fractions or aerosol iodine speciation (Gomez Martin-t02.docx).
Table S3. Statistics of soluble iodine speciation in bulk aerosol (given as fractions of TI and TSI)
Dataset S1. Compilation of field observations of total iodine, total soluble iodine, iodine enrichment in aerosol and soluble iodine speciation in aerosol in bulk, fine (PM_1 or $PM_{2.5}$) and coarse aerosol (Gomez Martin-ds01.docx).
Dataset S2. Compilation of field observations of mayor ions in fine (PM_1) and coarse aerosol (Gomez Martin-ds02.docx).

Introduction

The Supplementary Information consist of three individual tables containing information about the field campaigns considered in this work, as well as two spreadsheets containing the total iodine, total soluble iodine and iodine speciation data compiled from these campaigns, and the mayor ion data available for a subset of these campaigns. The main Supplementary File includes two supplementary texts describing data treatment and discussing details of the analytical methods employed in these campaigns to determine iodine speciation. It also includes eight supplementary figures related to the spatial variation of the total iodine size distribution and the total soluble iodine fraction, differen aspect of the spatial variation of the iodine speciation, and scatter plots of SOI versus selected mayor ions.

Supplementary Text 1: Data treatment

Besides concentration values at the detection limit for the three soluble species, some datasets contain negative SOI values (C6, C10, C14 and C17) and also SOI values with large relative uncertainty (C4, C6, C10, C17 and C20), mainly in the coarse aerosol fraction. We are aware of a debate in the literature about how to handle unreliable and unphysical concentration values (data with large errors or taking negative values) of calculated parameters such as SOI. Some authors argue for excluding data (negative or positive) with large uncertainties, while keeping negative values with small uncertainty, since removing such values would bias the dataset (Baker & Yodle, 2021). However, ignoring concentrations of SOI means that the rest of the speciation data of that particular station also has to be ignored as well, since the objective of this work is investigating interconversion processes between different species and their contribution to TSI.
For the purpose of the analysis reported in this work, which requires taking advantage of as much data as possible, the convention adopted has been to include all SOI data points with large relative uncertainty (2 in the fine fraction and 15 in the coarse fraction with relative uncertainty larger than 100%) and setting all negative SOI_{coarse} values to zero (18 values). The reasoning behind this convention is that both cases always occur for TSI ~ TII, i.e. SOI is effectively very close to zero. The negative values and the errors of unreliable SOI data relative to TSI are in most of the cases lower than 15%, which looks acceptable considering the uncertainties of the observations. Regarding the measurements at the detection limit, they are included in the analysis as they are. A spreadsheet containing the compiled data can be found in the Supplementary Information, where uncertainties are included and the values at the detection limit ad those that are negative in the original dataset are flagged.

Supplementary Text 2: The question of the iodine extraction method

Most studies report the use of ultrasonic agitation during aqueous extraction of iodine from the filters, in some cases over long periods of time (see Tables S1 and S2). However, it is known that ultrasonication leads to changes in aerosol iodine speciation (Baker et al.,

2000; Baker & Yodle, 2021; Yodle & Baker, 2019; Zhang et al., 2015) as a result of generation of H_2O_2 and other reactive oxygen species by acoustic cavitation (Kanthale et al., 2008), which depends both on agitation time and on sonic power (the latter is usually not reported). Moreover, speciation changes have been found to be larger for cellulose filters than for glass microfiber filters (Yodle & Baker, 2019). In the presence of H_2O_2, I^- is oxidized to HOI, which then may react with organics to form SOI.
All this raises the possibility that much of the published literature on aerosol iodine speciation may be unreliable. It has been argued that sample treatment may have contributed to the current lack of coherent understanding of the variability of aerosol iodine speciation observed in the field (Saiz-Lopez et al., 2012). However, there is no conclusive evidence relating differences between iodine speciation in different campaigns to the treatment of the samples. These differences may be also related to different ambient conditions. Hence, in this work we consider all the published data, with the caveat that measurements relying on long agitation time (see Table S1 and S2) or high sonication power may have overestimated SOI and underestimated iodide concentrations.

Supplementary Text 3: Hierarchical clustering

Hierarchical clustering analysis has been performed in order to classify similar aerosol iodine speciation and major aerosol ion variables in different groups or clusters. We use the Origin built-in clustering tools (OriginLab, n.d.). The analysis performed here uses the group average linkage method and the correlation distance. The distance is defined as 1-R (correlation) or 1 – |R| (absolute correlation), where R is the Pearson correlation coefficient, and it is calculated as the average distance between all pairs of objects in the different clusters (Hastie et al., 2009). Missing values are excluded in a pairwise manner to calculate the correlation. The data variables are classified in clusters for a minimum inter-cluster distance of 0.4 and plotted in a hierarchical tree plot called dendrogram (Figures S10-S11), which shows the distance at which two clusters merge. See chapter 14 of reference (Hastie et al., 2009) for further details about hierarchical clustering analysis.

Supplementary References

Baker, A. R., & Yodle, C. (2021). Indirect evidence for the controlling influence of acidity on the speciation of iodine in Atlantic aerosols. *Atmospheric Chemistry and Physics*, https://doi.org/10.5194/acp-2021-72.

Baker, A. R., Thompson, D., Campos, M. L. A. M., Parry, S. J., & Jickells, T. D. (2000). Iodine concentration and availability in atmospheric aerosol. *Atmospheric Environment*, *34*(25), 4331–4336. https://doi.org/https://doi.org/10.1016/S1352-2310(00)00208-9

Gómez Martín, J. C., Saiz-Lopez, A., Cuevas, C. A., Fernandez, R. P., Gilfedder, B., Weller, R., et al. (2021). Spatial and Temporal Variability of Iodine in Aerosol.

Journal of Geophysical Research: Atmospheres, *126*(9), e2020JD034410. https://doi.org/10.1029/2020JD034410

Hastie, T., Tibshirani, R., & Friedman, J. (2009). *The Elements of Statistical Learning*. New York, NY: Springer New York. https://doi.org/10.1007/978-0-387-84858-7

Kanthale, P., Ashokkumar, M., & Grieser, F. (2008). Sonoluminescence, sonochemistry (H2O2 yield) and bubble dynamics: Frequency and power effects. *Ultrasonics Sonochemistry*, *15*(2), 143–150. https://doi.org/10.1016/j.ultsonch.2007.03.003

OriginLab. (n.d.). Online help: 17.7.3.3 Algorithms (Hierarchical Cluster Analysis). Retrieved 23 March 2021, from https://www.originlab.com/doc/Origin-Help/HCA-Algorithm

Saiz-Lopez, A., Plane, J. M. C., Baker, A. R., Carpenter, L. J., von Glasow, R., Gómez Martín, J. C., et al. (2012). Atmospheric chemistry of iodine. *Chemical Reviews*, *112*(3). https://doi.org/10.1021/cr200029u

Yodle, C., & Baker, A. R. (2019). Influence of collection substrate and extraction method on the speciation of soluble iodine in atmospheric aerosols. *Atmospheric Environment: X*, *1*, 100009. https://doi.org/10.1016/j.aeaoa.2019.100009

Zhang, L., Hou, X., & Xu, S. (2015). Speciation Analysis of 129I and 127I in Aerosols Using Sequential Extraction and Mass Spectrometry Detection. *Analytical Chemistry*, *87*(13), 6937–6944. https://doi.org/10.1021/acs.analchem.5b01555

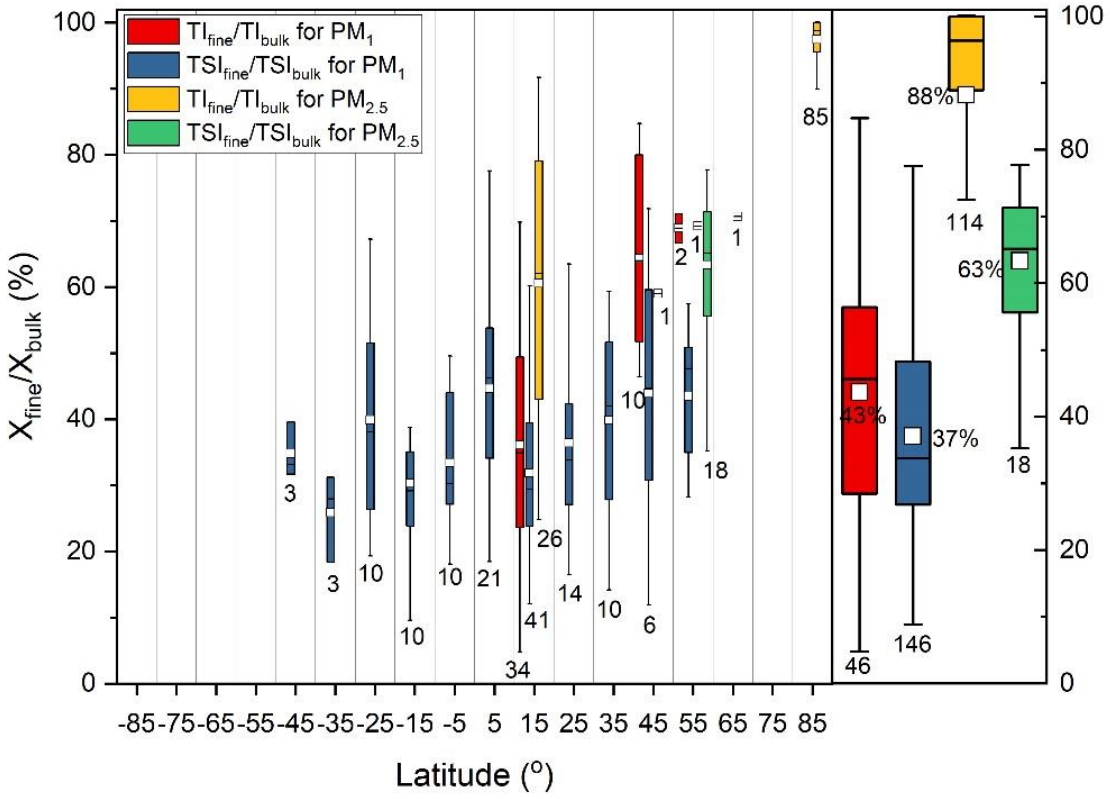

Figure S1. Left panel: Latitudinal dependence of the TI or TSI fraction in fine aerosol relative to bulk aerosol. Red and blue boxes represent the TI and TSI fractions in PM_1, while the yellow and green boxes are for $PM_{2.5}$. Right panel: global statistics of the TI and TSI fractions in PM_1 and $PM_{2.5}$. Box and whiskers plot statitistics as in Figure 2.

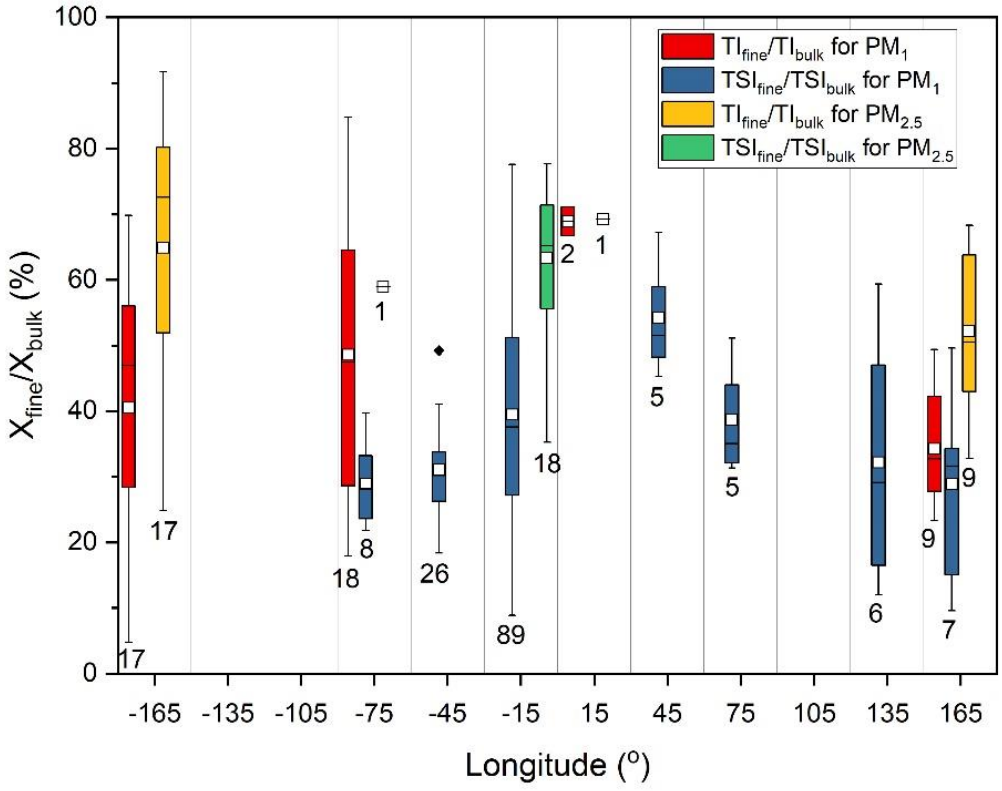

Figure S2. As Figure S1 but plotted as a function of longitude and excluding data outside the 60°S-60°N zonal band. Box and whiskers plot statitistics as in Figure 2.

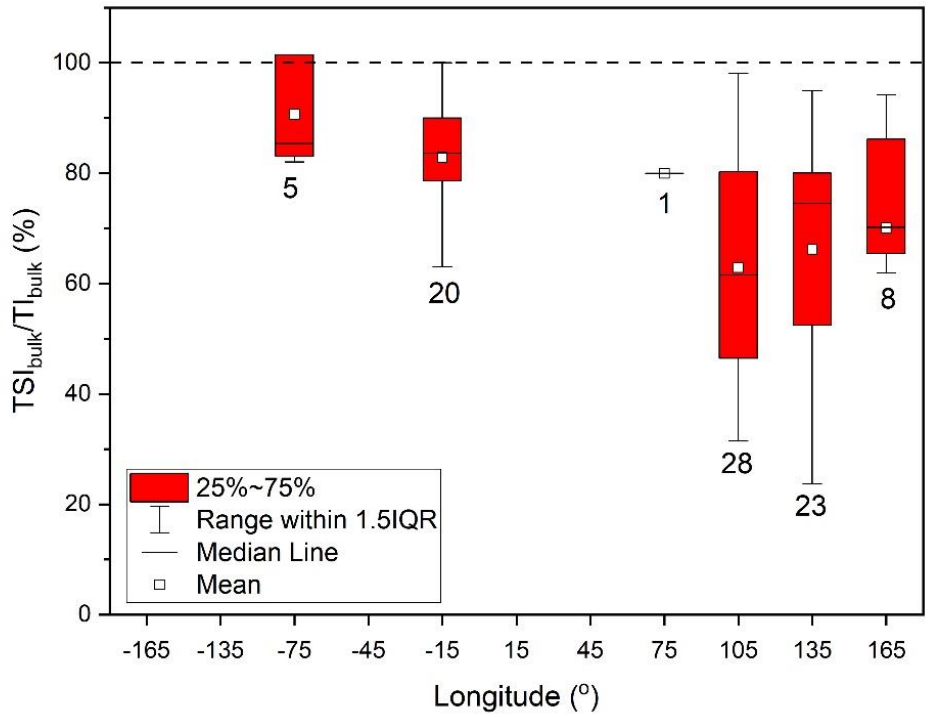

Figure S3. Longitudinal dependence of the TSI/TI ratio in bulk aerosol (zonal average between 60°S and 60°N). The 8 datapoints at the 15°E meridional band belong to station S35 (Riso, Dennmark, 56 °N). Box and whiskers plot statitistics as in Figure 2.

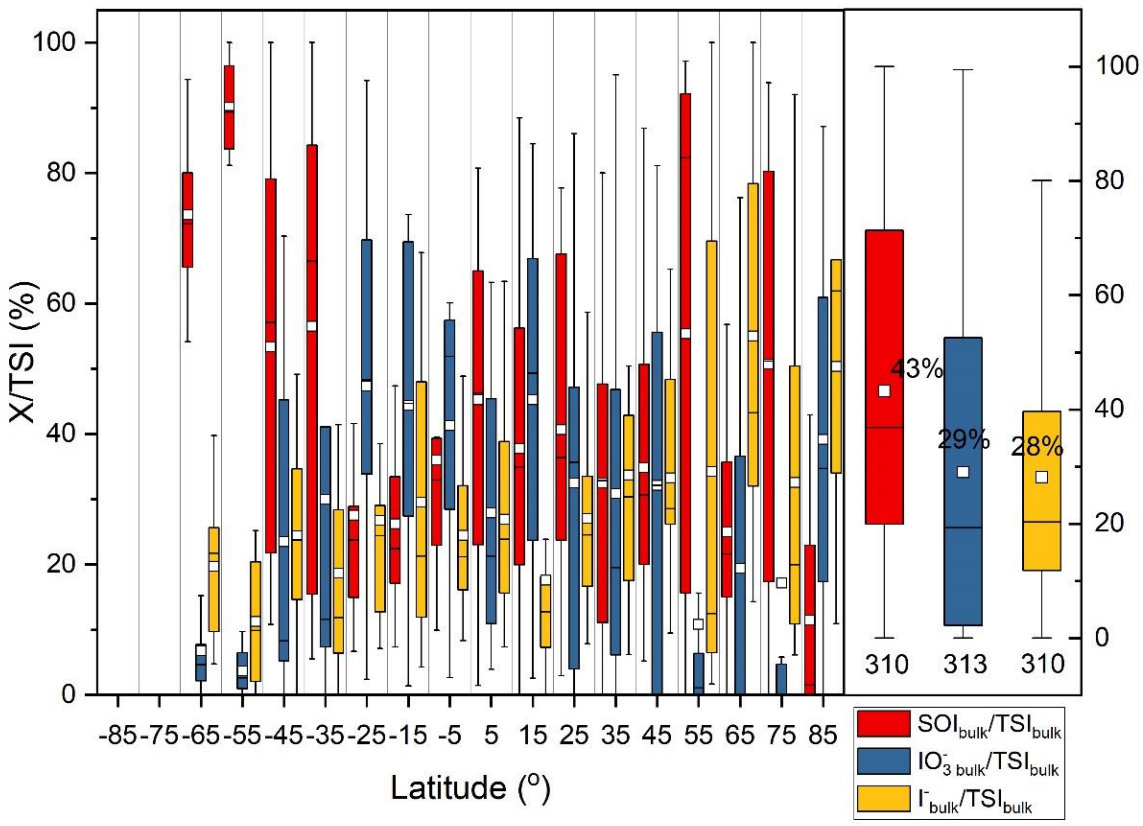

Figure S4. Left panel: Latitudinal dependence of the X to TSI ratio in bulk aerosol (red, blue and yellow boxes for X= SOI, IO_3^-, I^-, respectively). Right panel: global statistics of the X/TSI ratios in bulk aerosol (number of samples indicated). Box and whiskers plot statitistics as in Figure 2.

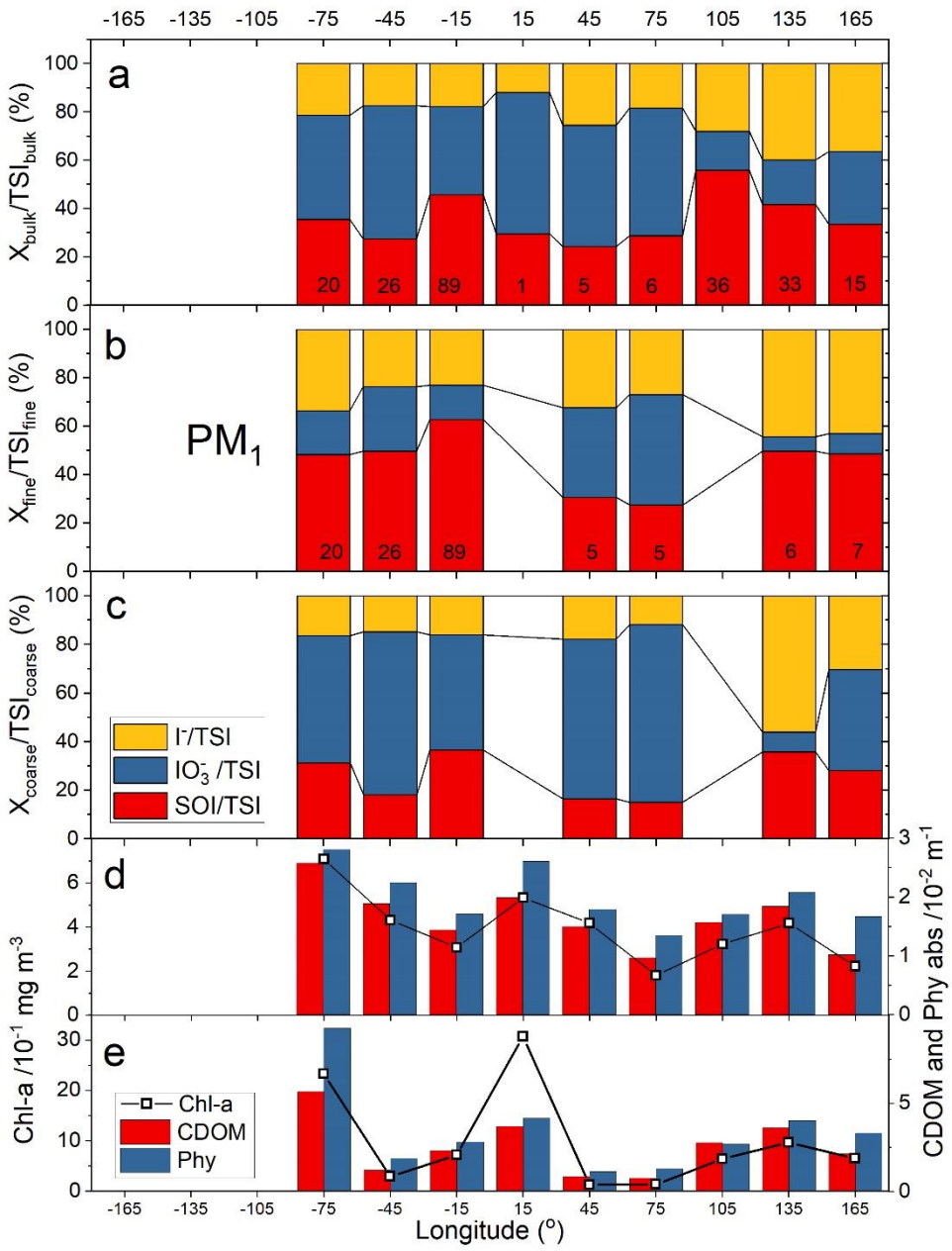

Figure S5. As Figure 2 for the longitudinal dependence of the X/TSI ratios in the 55°S-55°N zonal band, in bulk aerosol (panel a), and in the fine PM_1 (panel b) and coarse (panel c) aerosol fractions. The numbers at the bottom side of the bars indicate the number of observations. Panel c: Chlorophyll-a concentration (Chl-a, squares), CDOM and detritus absorption at 443 nm (CDOM, blue columns) and Phytoplankton absorption at 443 nm (Phyt, red columns) from the MODIS-A satellite mission. The satellite averages exclude data for land-locked seas where no measurements of iodine speciation exists (Baltic, Mediterranean, Caspian, Black, Red Seas and Persic Gulf). Panel d: as panel c for the specific coordenates of the campaings where iodine speciation was measured (averages in 1°x1° regions containing the coordinates of the campagins.)

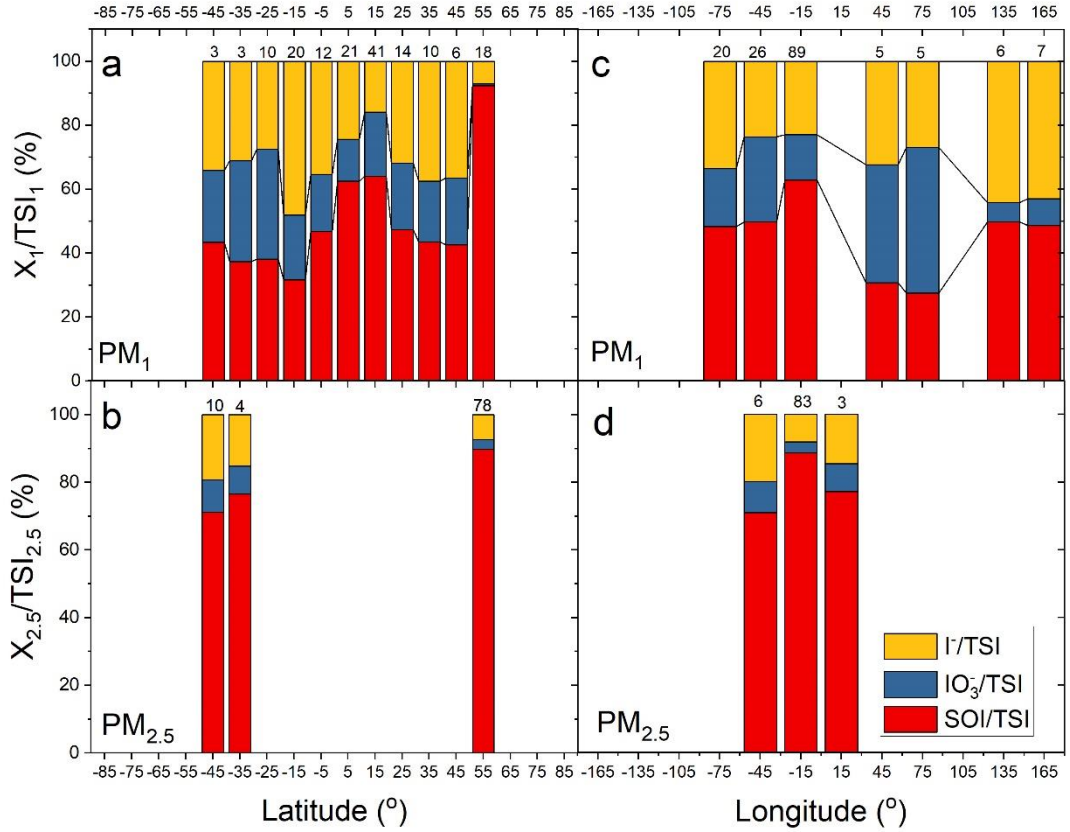

Figure S6. Latitudinal and longitudinal dependence of the soluble iodine speciation in fine aerosol. Panels a and b show the latitudinal dependence of iodide, iodate and SOI in PM_1 and $PM_{2.5}$, respectively. Panels c and d show the same but versus longitude (55°S-55°N). The numbers above the bars indicate the number of observations.

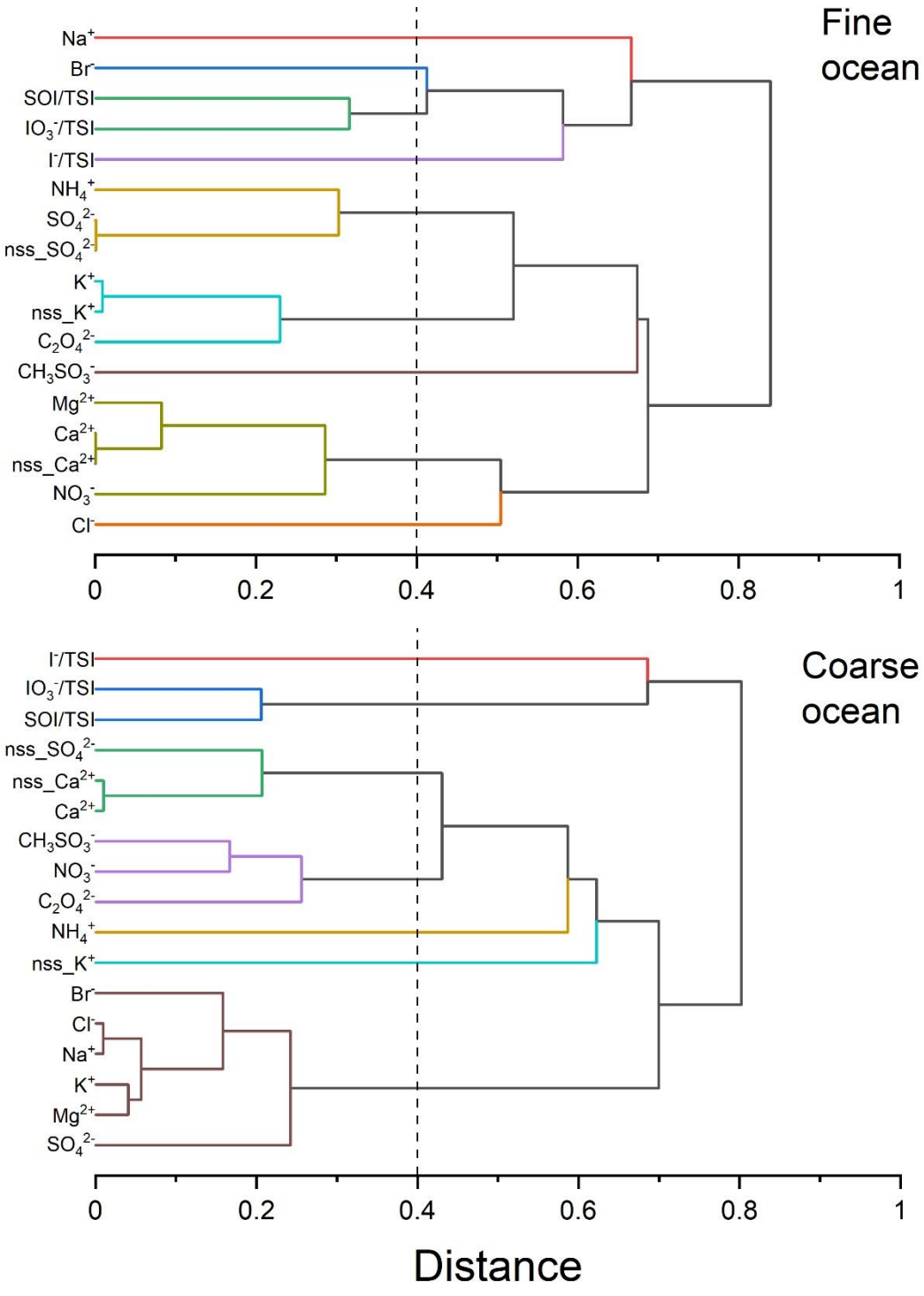

Figure S7. As Figure 5 for the open ocean data subset.

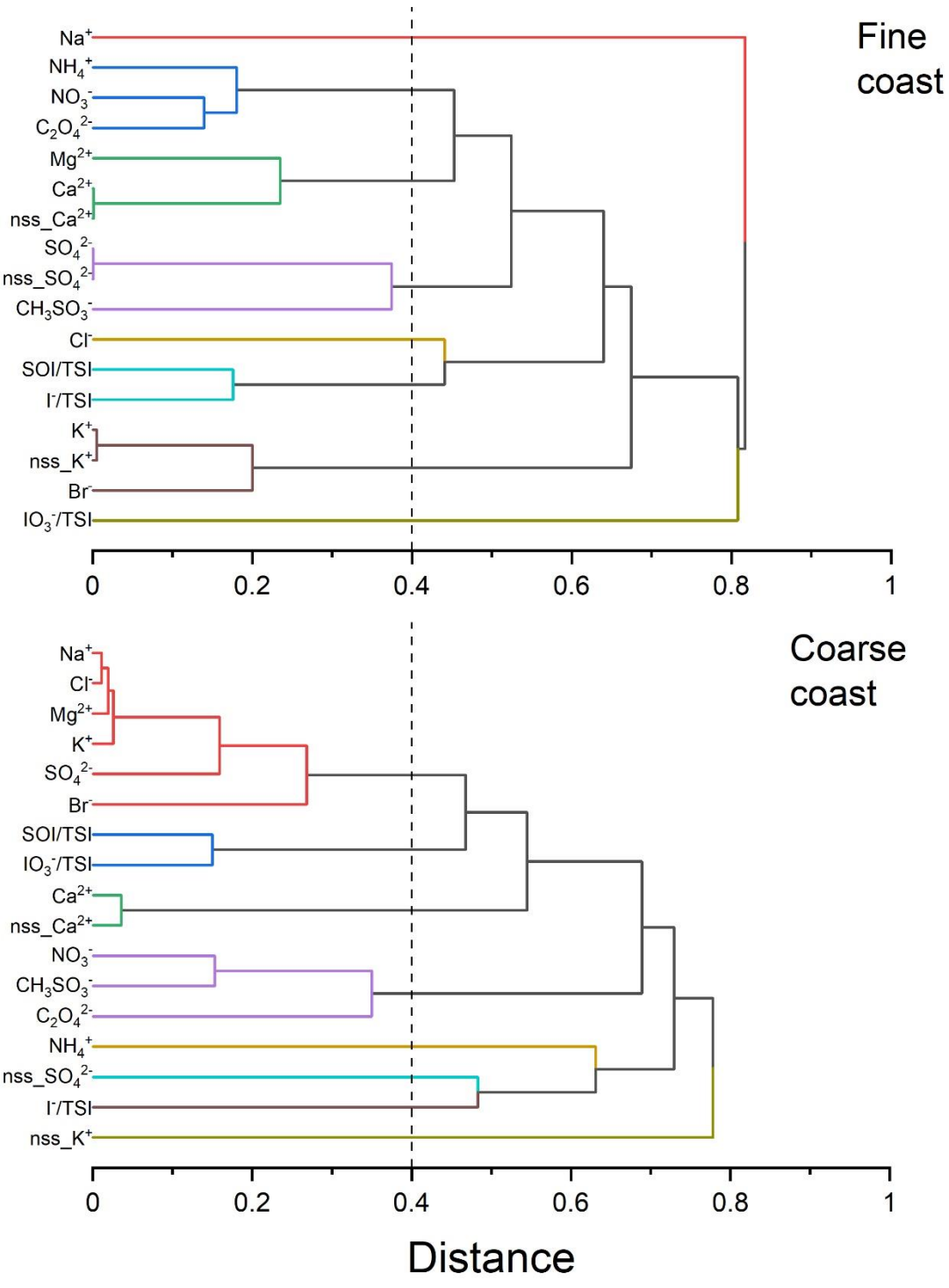

Figure S8. As Figure 5 for the coastal data subset.

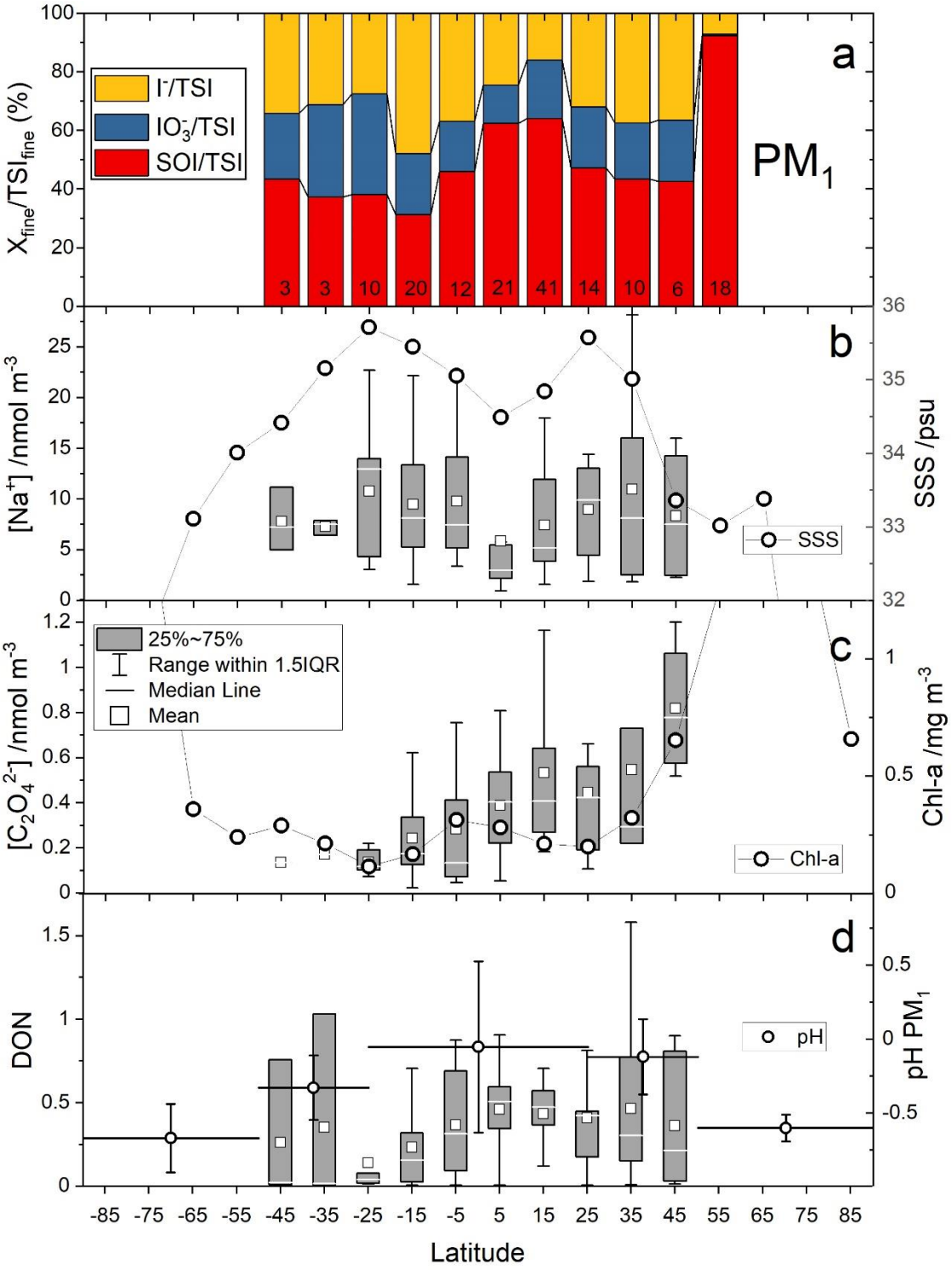

Figure S9. Latitudinal distribution of soluble iodine speciation in PM_1 (panel a), Na^+ concentration in PM_1 and Aquarius mission sea surface salinity (SSS) (panel b), oxalate concentration in PM_1 and sea surface chl-a (panel c), and degree of neutralization from MI observations and ATom campaign pH. Box and whiskers plot statitistics as in Figure 2.

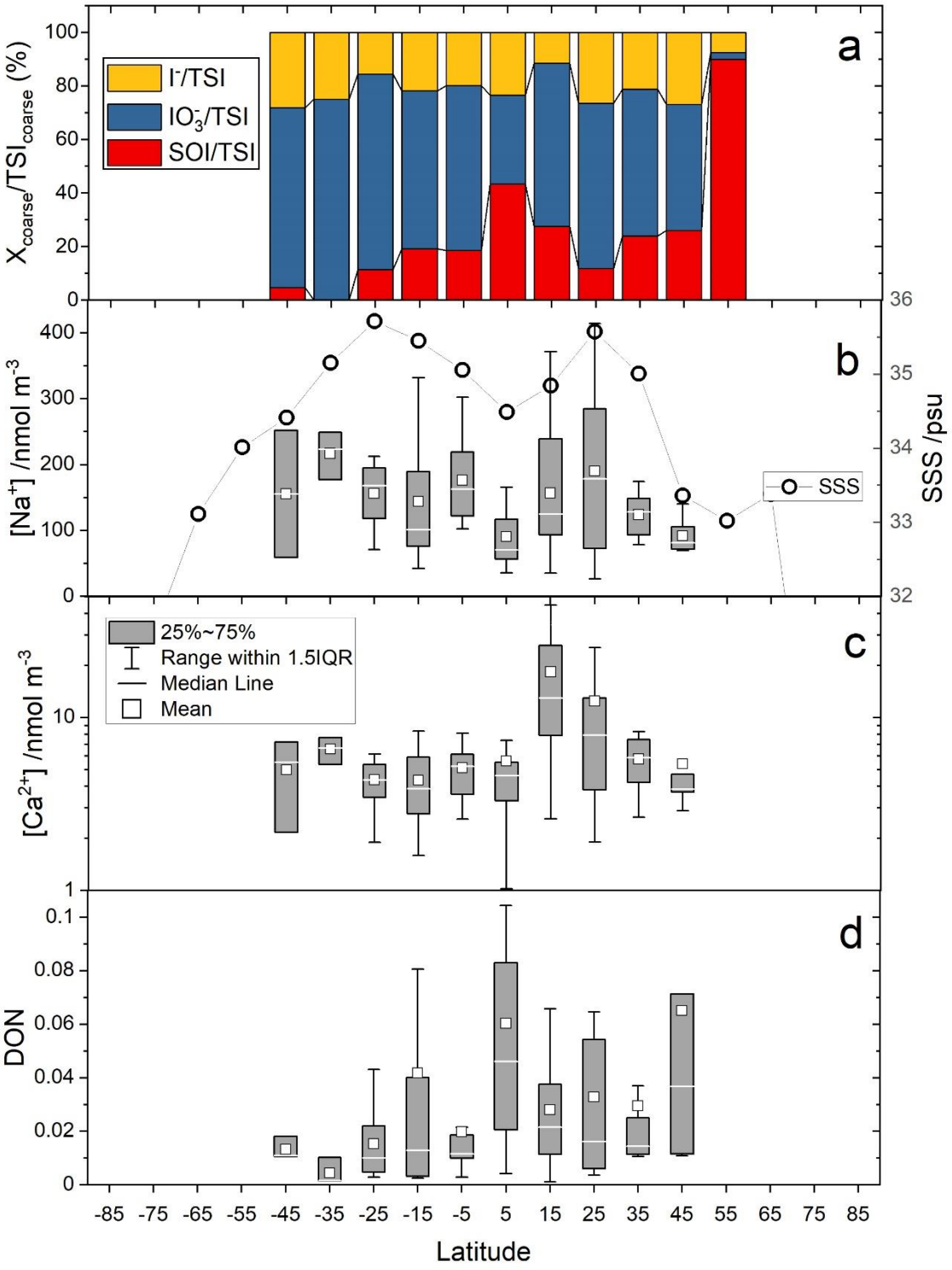

Figure S10. Latitudinal distribution of soluble iodine speciation in coarse aerosol (panel a), Na^+ concentration in coarse aerosol and Aquarius mission sea surface salinity (SSS) (panel b), Ca^{2+} concentration in coarse aerosol (panel c), and degree of neutralization from MI observations. Box and whiskers plot statitistics as in Figure 2.